The CH_3CHOO 'Criegee intermediate' and its anion: isomers, infrared spectra, and W3-F12 energetics

M. Kettner A. Karton A. J. McKinley D. A. Wild*

School of Chemistry and Biochemistry, The University of Western Australia, M310, 35 Stirling Hwy, Crawley, Australia 6009.

*duncan.wild@uwa.edu.au

Abstract: For the CH_3CHOO Criegee intermediates (ethanal-oxide) and analogous anions, we obtain heats of formations and electron affinities at CCSDT(Q)/CBS level of theory by means of the high-level W3-F12 thermochemical protocol. The electron affinities amount to 0.20 eV and 0.35 eV for the *cis* and *trans* isomer, respectively. Neutral *cis* and *trans* isomers are separated by 14.1 kJ mol^{-1}, the anions are almost isoenergetic (0.4 kJ mol^{-1} separation). Harmonic vibrational frequencies are presented at CCSD(T)/aug′-cc-pVTZ level of theory. Since the synthesis of these species in gas-phase experiments might be possible in the near future, we include a predicted photoelectron spectrum.

Introduction

Carbonyl oxides, also known as Criegee Intermediates (CI), are understood to be linking structures in tropospheric ozonolysis reactions.[1] During collisions between unsaturated hydrocarbons and ozone in earth's atmosphere, these short-lived, zwitterionic molecules provide a pathway to the formation of ·OH radicals through unimolecular decomposition.[2–6] As one of the main gas-phase oxidants in our atmosphere, it is also likely to react with other carbonyl oxides as well as H_2O, SO_2, NO, NO_2, other alkenes or ozone molecules,[7–11] only to name a few examples for the rich chemistry these molecules exhibit.

It is this multitude of reactions that raises our curiosity towards such a rather unstable molecule, recently fuelled even more so by the discovery of alternate methods for gas-phase synthesis for the simplest of all CIs, the methanal-oxide (MO).[8,12] In one of these reactions, Welz and co-workers showed that CH_2OO can be obtained through photolysis of CH_2I_2 in the presence of O_2.[8] As a consequence, the behaviour of the intermediate could now be investigated utilising various spectroscopic methods, such as UV adsorption and gas-phase IR experiments;[13,14] yet due to its metastable nature, experiments on MO are indeed rather challenging. However, the small size of the intermediate allows for a thorough theoretical analysis.[15] For instance, Fang et al. studied the potential energy surface of the reaction of CH_2 and O_2 on the singlet and triplet surfaces using CASSCF-type calculations.[16] Nguyen et al.[17] obtained the heat of form-

ation and ionisation energy of the Criegee intermediate at the CCSD(T)/CBS level using W1 theory.[18]

In natural atmospheric processes, the precursors to CI formation—volatile organic compounds (VOC)—are for example generated by our forests and as earth's biosphere slowly warms more VOCs can enter the carbonyl cycle.[19] The reaction of VOCs with ozone creates CIs with high internal energy, most of which immediately dissociate through unimolecular rearrangements leading to, amongst others, ·OH molecules.[15] CIs stable enough to participate in further reactions (lifetimes of approx. 100 ms were postulated), are often called stabilised Criegee Intermediates (sCI).[2,20]

The main focus of current and past research lies within the neutral CI chemistry. However, it is also possible to explore the neutral CIs coming from an anionic surface via anion photoelectron spectroscopy. Recently, our group presented the first theoretical anionic structure for the simplest of all carbonyl oxides (MO) and found that it is stable with respect to dissociation[21] In this paper, we would like to discuss the neutral and anionic properties of the ethanal-oxide. Due to its β-carbon, it seems more important to atmospheric precesses than its 'simpler' counterpart.[6,19]

Computational Methods

The geometries and harmonic frequencies of the anion and neutral CH_3CHOO species were obtained at the CCSD(T)/aug′-cc-pVTZ level of theory (where aug′ indicates the use of aug-cc-pVTZ on O and C and cc-pVTZ on H).[22,23] All the high-level ab initio calculations were performed using the Cfour and Molpro program suites.[24,25]

The total atomisation energies at the bottom of the well (TAE_e) of the CH_3CHOO and CH_3CHOO^- species are obtained by means of the W3-F12 procedure.[26] W3-F12 theory combines F12 methods[27,28] with extrapolation techniques in order to reproduce the CCSDT(Q) basis set limit energy.

The CCSD(T)/CBS energy is obtained from the W2-F12 theory and the post-CCSD(T) contributions are obtained from W3.2 theory.[29,49] In brief, the Hartree–Fock component is calculated with the VQZ-F12 basis set (VnZ-F12 denotes the cc-pVnZ-F12 basis sets of Peterson et al. which were developed for explicitly correlated calculations).[30] Note that the complementary auxiliary basis (CABS) singles correction is included in the SCF energy.[31–33] The valence CCSD-F12 correlation energy is extrapolated from the VTZ-F12 and VQZ-F12 basis sets, using the $E(L) = E_\infty + A/L^\alpha$ two-point extrapolation formula, with $\alpha = 5.94$. In all of the explicitly-correlated coupled cluster calculations the diagonal, fixed-amplitude 3C(FIX) ansatz[31,34,35] and the CCSD-F12b approximation[32,36] are employed. The quasiperturbative triples, (T), corrections are obtained from standard CCSD(T) calculations (i.e., without inclusion of F12 terms) and scaled by the factor $f = 0.987 \cdot E^{\mathrm{MP2-F12}}/E^{\mathrm{MP2}}$. This approach has been shown to accelerate the basis set convergence.[26,36]

The higher-order connected triples, $T_3 - (T)$, valence correlation contribution is extrapolated from the cc-pVDZ and cc-pVTZ basis sets using the above two-point extrapolation formula with $\alpha = 3$, and the parenthetical connected quadruples contribution (CCSDT(Q)−CCSDT) is calculated with the cc-pVDZ basis set.[29] The CCSD inner-shell contribution is calculated with the core-valence weighted correlation-consistent A′PWCVTZ basis set of Peterson and Dunning,[37] whilst the (T) inner-shell contribution is calculated with the PWCVTZ(no f) basis set (where A′PWCVTZ indicates the combination of the cc-pVTZ basis set on hydrogen and the aug-cc-pwCVTZ basis set on carbon, and PWCVTZ(no f) indicates the cc-pwCVTZ basis set without the f functions).[26]

The scalar relativistic contribution (in the second-order Douglas–Kroll–Hess approximation[38,39]) is obtained as the difference between non-relativistic CCSD(T)/A′VDZ and relativistic CCSD(T)/A′VDZ-DK calculations (where A′VDZ-DK indicates the combination of the cc-pVDZ-DK basis set on H and aug-cc-pVDZ-DK basis set on C and O).[40] The atomic spin-orbit coupling terms are taken from the experimental fine structure, and the diagonal Born–

Oppenheimer corrections (DBOC) are calculated at the HF/cc-pVTZ level of theory. The zero-point vibrational energies (ZPVEs) are derived from the harmonic frequencies (calculated at the CCSD(T)/A′VTZ level of theory for the CH_3CHOO and CH_3CHOO^- species.

The total atomisation energies at 0 K (TAE_0) are converted to a heats of formation at 298 K using the Active Thermochemical Tables (ATcT)[41–43] atomic heats of formation at 0 K (H 216.034(1) kJ mol^{-1}, C 711.38(6) kJ mol^{-1}, and O 246.844(2) kJ mol^{-1}), and the CODATA[44] enthalpy functions, $H_{298} - H_0$, for the elemental reference states (H_2(g) = 8.468(1) kJ mol^{-1} and C(*cr*,graphite) = 1.050(20) kJ mol^{-1}), while the enthalpy functions for the CH_3CHOO and CH_3CHOO^- species are obtained within the ridged rotor harmonic oscillator (RRHO) approximation from B3LYP/A′VTZ geometries and harmonic frequencies.[45–47]

Anion photoelectron spectra were simulated by determining the Franck–Condon Factors (FCFs) linking the anion and neutral CH_3CHOO species vibrational states. FCFs were calculated using the ezSpectrum 3.0 program which is made freely available by Mozhayskiy and Krylov.[48] The program produces FCFs by undertaking Duschinsky rotations of the normal modes between states. Input to the code consists of the output from the ab initio calculations, being geometries, vibrational frequencies, and vibrational normal mode vectors. The predicted stick spectra were convoluted with a Gaussian response function of width 0.002 eV to simulate an experimental spectrum.

Results and Discussion

Geometries and vibrational frequencies

In Figure 1, the four ethanal-oxide structures are presented. The neutral, closed-shell equilibrium isomers, *cis*-ethanal-oxide (EO1) and the *trans*-ethanal-oxide (EO2), both feature C_S symmetry. Due to the electrotatic interaction between H_c and H_d atom of the methyl group with the O_b atom, EO1 is by 14.1 kJ mol^{-1} more stable than EO2. A partial charge representation of a natural population analysis is illustrated in Figure S1 of the supporting information. The analogous anionic structures of EO1 and EO2 are labelled as AEO1 and AEO2, respectively. Contrary to the neutrals, these structures do not show any symmetry, which can be seen when comparing the dihedral angles ϕ_1 and ϕ_2 in Figure 1. It is also noticed that the AEO2 isomer is slightly more stable (by 0.4 kJ mol^{-1}) than the AEO1 isomer. For both anionic structures, the C−C bond is lengthened on average by 2 pm, the C−O bond by 7 pm and the O−O bond by 10 pm, compared to their neutral counterparts.

The calculated EO1 geometry is in good agreement with the B3LYP/6-31G(d,p) structure reported by Gutbrod and co-workers,[6] where the largest difference is the C−O−O angle, deviating by 1.0°. Both, the EO1 and EO2 geometries also compare well to the neutral form of the simplest carbonyl oxide, methanal-oxide (MO), where the CCSD(T)/A′VQZ geometry was taken from Ref. [21]), which shows very similar bond lengths [r(C−O) = 1.270 Å, r(O−O) = 1.343 Å and θ(C−O−O) = 117.9°].

To the best of our knowledge, the is the first published geometry of AEO1 and AEO2. Both however display similar structural features as the anionic form of methanal-oxide (AMO), which exhibits bond lengths of r(C−O) = 1.334 Å and r(O−O) = 1.450 Å; and bond angles of θ(C−O−O) = 111.7°, ϕ_1 = 164.8° and ϕ_2 = −17.9°.[21]

A natural bond orbital (NBO) analysis suggests that the anionic structures harbour the additional electron in the C_b lone-pair orbital, which explains the change from C_1 to C_S symmetry when going from the neutral to the anion. Additionally, the C_a−C_b bond is weakened significantly as the summed occupancies of these double bonding orbitals drop from ca. 4.0 for the neutrals to ca. 3.0 in the anions. The remaining electron populates a O_a lone pair orbital, which also reveals why the O_a−O_b bond is longer for the anion. It should be noted however that the C_b−O_a bond orbital and the O_a lone pair orbital are almost degenerate. Compared to the MO and AMO electronic structures, the neutrals and anions are very similar; yet due to the methyl group, the C_b−O_a anti-bonding or-

Figure 1 | Anion and neutral species of CH_3CHOO. Bond lengths are given in Ångström. ϕ_1 refers to the dihedral angle between C_a, C_b, O_a and O_b; ϕ_2 between H_a, C_b, O_a and O_b. All geometric parameters obtained from CCSD(T)/A′VTZ calculations. The full geometric data are presented in Table S1 of the supplementary information.

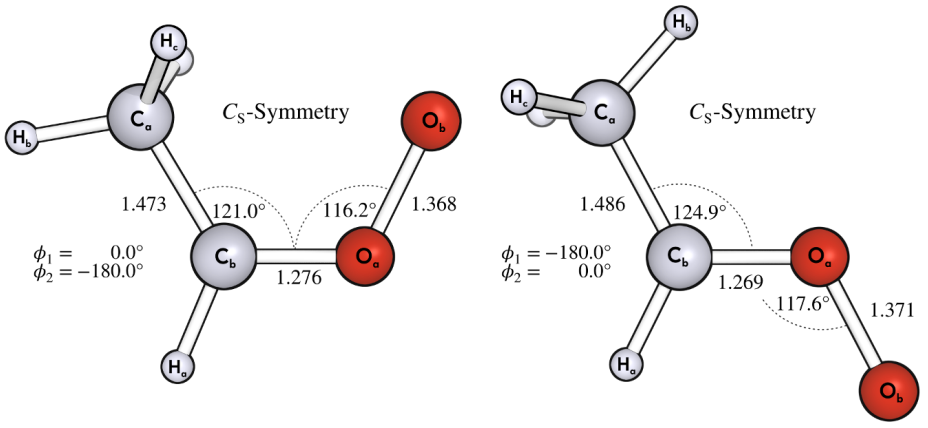

EO1: *cis*-ethanal-oxide (neutral) **EO2**: *trans*-ethanal-oxide (neutral)

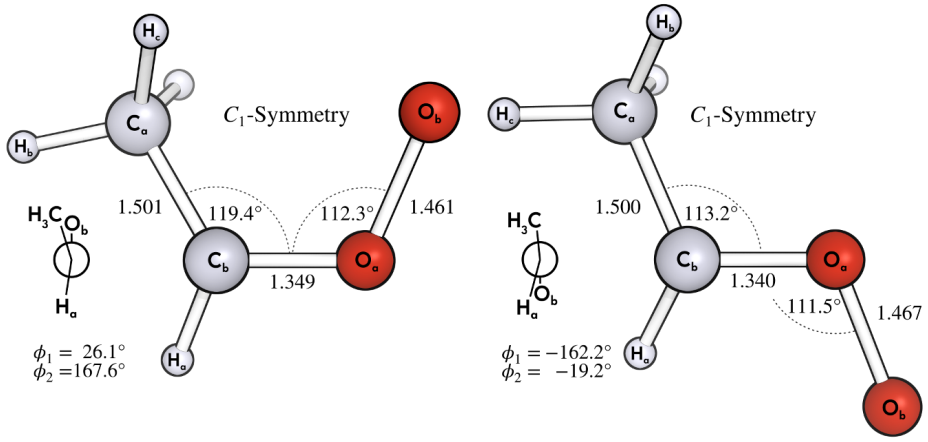

AEO1: *cis*-ethanal-oxide (anion) **AEO2**: *trans*-ethanal-oxide (anion)

bitals in the ethanal-oxide species display slightly higher electron density. The detailed NBO analysis and comparison between the carbonyl oxide structures can be found in Table S2 of the supporting information.

The Vibrational data sets are presented in Table 1, where they are sorted in accordance to the standard numbering scheme for the C_S point group. In the neutral structures, EO1 exhibits a weak interaction of the terminal oxygen O_b and the methyl hydrogen atoms H_c and H_d. Similar to a weak hydrogen bond, this interaction stabilises the molecule by 14.1 kJ mol^{-1}, compared to EO2. This is also the cause why all the vibrations where O_b, H_c and H_d are involved are red-shifted in EO2. The most notable case is the C−C−O−O out-of-plane twisting (ν_{17}) which shows an eigenfrequency of 442.9 cm^{-1} in EO1 and 247.8 cm^{-1} in EO2. Another example is the methyl wagging / O−O−C bend (ν_{11}) where the red-shift amounts to 115.5 cm^{-1}. In contrast, the C_b−H_a wagging/methyl rocking vibration (ν_{16}) is blue-shifted by 119.8 cm^{-1}.

The differences in mode frequencies between the anionic and neutral seem quite similar to the the differences we encountered in the AMO. Reflecting the increased stability, the O−O stretches (ν_{10}) blue-shift on average by 114 cm^{-1}, when comparing the anion to the neutral. It can be seen however, that the blue-shift for the asymmet-

Table 1 | Computed harmonic vibrational data of the CH_3CHOO anion and neutral species at the CCSD(T)/A′VTZ level of theory. The ordering of the modes of all other species has been changed to reflect that of EO1, for direct comparison.

Mode	Neutral			Anion			Mode description
	EO1	EO2	Sym.	AEO1	AEO2	Sym.	
ν_1	3201.3	3165.7	a'	3050.8	3104.4	a	C_b–H_a stretch
ν_2	3155.4	3146.7	a'	3090.2	3015.3	a	C_a–H asymmetric stretch (methyl group)
ν_3	3025.7	3034.5	a'	2918.0	2886.1	a	C_a–H symmetric stretches (methyl group)
ν_4	1514.2	1524.5	a'	1492.5	1381.1	a	asymmetric O–C/C–O stretch
ν_5	1469.8	1461.8	a'	1401.6	1500.2	a	CH_2 scissor / H_b–C_aC_b bend
ν_6	1397.0	1418.8	a'	1361.5	1348.4	a	methyl inversion / C–O stretch
ν_7	1305.9	1312.3	a'	1230.7	1245.2	a	in-plane C_b–H_a rocking/ C–O stretch
ν_8	1113.4	1155.2	a'	1117.9	1118.4	a	methyl wagging / C–C stretch
ν_9	973.8	942.4	a'	913.3	937.7	a	C–C stretch
ν_{10}	904.9	894.8	a'	786.8	784.8	a	O–O stretch
ν_{11}	668.8	553.3	a'	526.3	477.7	a	methyl wagging / O–O–C bend
ν_{12}	303.9	319.9	a'	220.6	302.3	a	C–C–O–O scissor bend/deformation
ν_{13}	3079.4	3097.6	a''	3018.2	3064.8	a	C_a–H asymmetric stretch (methyl group)
ν_{14}	1454.1	1479.9	a''	1445.9	1466.8	a	CH_2 twist / C_a–H_b rocking
ν_{15}	1034.1	1053.5	a''	1025.6	1029.6	a	methyl twisting / C_b–H_a rocking
ν_{16}	723.7	843.4	a''	648.6	654.2	a	C_b–H_a wagging / methyl rocking
ν_{17}	442.9	247.8	a''	305.6	120.4	a	C–C–O–O out-of-plane twisting
ν_{18}	209.0	153.4	a''	159.0	195.5	a	methyl twisting (internal rotation)

All frequencies are given in cm^{-1}.

ric O–C / C–O stretch (ν_4) is much larger when going from AEO2 to EO2 than when going from AEO1 to EO1.

W3-F12 components and Electron affinity

The components of the W3-F12 total atomisation energies for the ethanal-oxide species are given in Table S3 of the supporting information. At the W2-F12 level, the relativistic, all-electron CCSD(T) contributions to TAE_0 add up to 2746.5 kJ mol^{-1} (EO1), 2724.0 kJ mol^{-1} (AEO1), 2747.2 kJ mol^{-1} (EO2) and 2709.5 kJ mol^{-1} (AEO2).

The generally good performance of the CCSD(T)/CBS level of theory in computational thermochemistry can typically be attributed to the large degree of cancellation between higher-order triples contributions, $T_3 - (T)$, and post-CCSDT contributions. For systems dominated by dynamical correlation, these contributions are of similar magnitude, however, the $T_3 - (T)$ excitations tend to universally decrease the atomisation energies whereas the post-CCSDT excitations tend to universally increase the atomisation energies. In the present case, we notice an overall post-CCSD(T) contribution to the atomisation energy of 5.5 kJ mol^{-1} for the neutral structures 1.8 kJ mol^{-1} for the anions. $T_4 - (Q)$, is likely to reduce the magnitude of the connected quadruple excitations, and therefore our CCSDT(Q)/CBS values should be regarded as upper limits of the TAEs.

The heats of formation for the neutral species at 0 K amount to 51.3 kJ mol^{-1} (EO1) and 65.4 kJ mol^{-1} (EO2) At 298 K we report heats of formation of 37.8 kJ mol^{-1} (EO1) and 52.6 kJ mol^{-1} (EO2). For the anionic structures the following heats of formation were obtained: 32.2 kJ mol^{-1} (AEO1) and 31.7 kJ mol^{-1} (AEO2) at 0 K; as well as 20.1 kJ mol^{-1} (AEO1) and 20.0 kJ mol^{-1} (AEO2) at 298 K.

Using the W3-F12 heats of formation for the CH_3CHOO neutral and anion species, we were able to calculate the anion electron affinities, the components of which are presented in Table 2. For the EO1 ← AEO1, the electron affinity amounts to 19.1 kJ mol^{-1} at 0 K and 17.7 kJ mol^{-1} at 298 K; for the EO2 ← AEO2 transition, we found an electron affinity of 33.6 kJ mol^{-1} at 0 K and 32.6 kJ mol^{-1} at 298 K. It is noted that the post-CCSD(T) contributions to the electron affinity add up to as much

as 3.3 kJ mol^{-1} and 4.1 kJ mol^{-1} for the EO1 ← AEO1 and EO2 ← AEO2 transitions, respectively.

Table 2 | Component breakdown of the W3-F12 electron affinities E_{EA} of the ethanal-oxide oxide isomers.

Property	E_{EA}(EO1 ← AEO1)	E_{EA}(EO2 ← AEO2)
SCF	−17.3	−7.9
CCSD	41.7	46.8
(T)	−8.4	−7.1
T_3 − (T)	1.1	0.6
(Q)	−4.4	−4.7
Inner-Shell	−0.6	−0.5
Rel.	−0.3	−0.3
DBOC	−0.3	−0.2
TAE_e	11.5	26.6
ZPVE	−7.6	−7.0
TAE_0	19.1	33.6
$\Delta H_{f,0}$	19.1	33.6
$\Delta H_{f,298}$	17.7	32.6

All energies are given in kJ mol^{-1}.

Predicted anion photoelectron spectra

If the anionic forms of the ethanal-oxide can be synthesised, it should be possible to measure their anionic photoelectron spectra. The main transitions should be the EO1 ← AEO1 transition (T1) and the EO2 ← AEO2) transition (T2). These spectra were simulated employing the ezSpectrum 3.0 code using the geometries, vibrational frequencies, and normal mode vectors of a CCSD(T)/A′VTZ harmonic calculation For both simulations, the temperature was set to 10 K, which is appropriate for species entrained in a molecular beam produced via supersonic expansion. Up to 10 quanta were allowed in each excited state vibrational mode (i.e. the modes of the neutral CH_3CHOO species). The predicted photoelectron spectra, applying the Duschinsky approach, are presented in Figure 2, where the grey part of the spectrum marks the combination bands, whereas the red part represents the pure progressions; together they form the fully predicted spectrum. To provide a clearer picture of what an experimental spectrum might look like, we the convoluted the stick spectra with a Gaussian response function whose full width at half maximum was set to 0.002 eV and the resulting simulated spectrum is shown in Figure S2 of the supporting information.

Figure 2 | Predicted anion photoelectron stick spectra (red marks the pure progressions) for both transitions (Simulated using the Duschinsky approach. Here, E_{eB} is the electron binding energy.

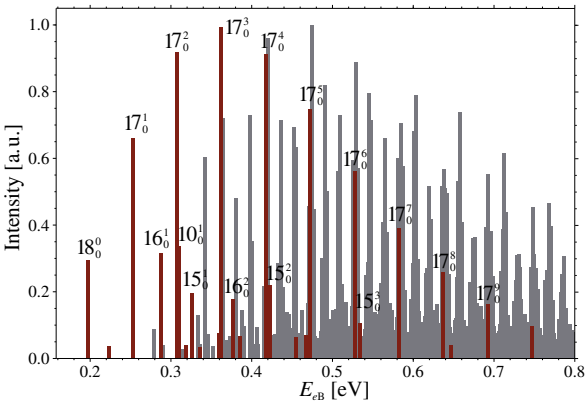

T1: EO1 ← AEO1

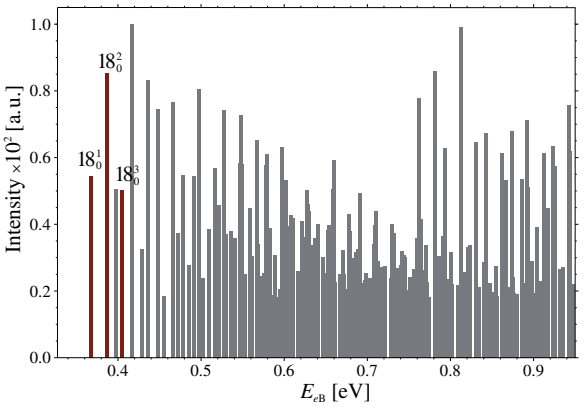

T2: EO2 ← AEO2

During the T1 transition, the geometry only changes slightly and most of the normal modes can be cast onto the neutral system. The determinant of the normal modes rotation matrix: |Det($\boldsymbol{S}$)| is 0.98. For the T2 transition, |Det($\boldsymbol{S}$)| is 0.88, yielding much lower transition intensities (on the order of 10^2 times lower).

Most of the the pure T1 transitions are due to ν_{17}, the C−C−O−O out-of-plane twisting mode. Other main contributors to the T1 spectrum are the O−O stretch mode ν_{10}, methyl twisting / C_b−H_a rocking mode ν_{15}, C_b−H_a wagging / methyl rocking mode ν_{16} and the methyl twisting mode ν_{18}. The single most important pure progression in the T2 spectrum is the methyl twisting mode ν_{18};

this methyl group is rotated during the transition. In general, these observations are consistent with the shifts in vibrational frequencies and changes in geometry during the transition.

Conclusion

In summary, we show that two different anions, a *cis* and *trans* form, of the ethanal-oxide exist. They both have a similar geometry and a somewhat similar vibrational structure compared to their corresponding neutral counterparts. By means of the high-level W3-F12 thermochemical protocol we found the electron to be bound by 0.20 eV and 0.35 eV, for the *cis*- and *trans*-ethanal-oxide anion, respectively. While the neutral *cis* and *trans* isomers are separated by 14.1 kJ mol^{-1} (the *cis* form is more stable than the *trans* isomer), the anions are separated by an negligible amount of 0.4 kJ mol^{-1} (here the *trans* form is more stable). The major geometric differences between the anion and neutral are the increased C−O and O−O bond lengths, as well as the change of symmetry, from a C_S point group for the neutrals to C_1 in the anions. Anion photoelectron spectra of transitions between these structures were also simulated. Combined with our IR-frequencies, these spectra provide a sound foundation for an analysis of ethanal-oxide structures in future gas-phase experiments.

Acknowledgements

We gratefully acknowledge an Australian Research Council (ARC) Discovery Early Career Researcher Award (to A.K., project number: DE140 100 311) and the generous allocation of computing time from the National Computational Infrastructure (NCI) National Facility.

References

[1] R. Criegee and G. Wenner. “Die Ozonisierung des 9,10-Oktalins”. In: *Justus Liebigs Annalen der Chemie* 564.1 (1949), pp. 9–15. ISSN: 1099-0690. DOI: 10.1002/jlac.19495640103.

[2] G. T. Drozd, J. Kroll, and N. M. Donahue. “2,3-Dimethyl-2-butene (TME) Ozonolysis: Pressure Dependence of Stabilized Criegee Intermediates and Evidence of Stabilized Vinyl Hydroperoxides”. In: *The Journal of Physical Chemistry A* 115.2 (2011), pp. 161–166. DOI: 10.1021/jp108773d.

[3] D. Johnson and G. Marston. “The gas-phase ozonolysis of unsaturated volatile organic compounds in the troposphere”. In: *Chemical Society Reviews* 37 (4 2008), pp. 699–716. DOI: 10.1039/B704260B.

[4] A. S. Hasson, K. T. Kuwata, M. C. Arroyo, and E. B. Petersen. “Theoretical studies of the reaction of hydroperoxy radicals (HO_2) with ethyl peroxy ($CH_3CH_2O_2$), acetyl peroxy ($CH_3C(O)O_2$), and acetonyl peroxy ($CH_3C(O)CH_2O_2$) radicals”. In: *Journal of Photochemistry and Photobiology A: Chemistry* 176.1–3 (2005), pp. 218–230. ISSN: 1010-6030. DOI: 10.1016/j.jphotochem.2005.08.012.

[5] R. Gutbrod, R. N. Schindler, E. Kraka, and D. Cremer. “Formation of OH radicals in the gas phase ozonolysis of alkenes: the unexpected role of carbonyl oxides”. In: *Chemical Physics Letters* 252.3-4 (Apr. 1996), pp. 221–229. ISSN: 0009-2614. DOI: 10.1016/0009-2614(96)00126-1.

[6] R. Gutbrod, E. Kraka, R. N. Schindler, and D. Cremer. “Kinetic and Theoretical Investigation of the Gas-Phase Ozonolysis of Isoprene: Carbonyl Oxides as an Important Source for OH Radicals in the Atmosphere”. In: *Journal of the American Chemical Society* 119.31 (1997), pp. 7330–7342. DOI: 10.1021/ja970050c.

[7] Y.-T. Su, H.-Y. Lin, R. Putikam, H. Matsui, M. C. Lin, and Y.-P. Lee. “Extremely rapid self-reaction of the simplest Criegee intermediate CH_2OO and its implications in atmospheric chemistry”. In: *Nature Chemistry* 6.6 (Mar. 2014), pp. 477–483. DOI: 10.1038/nchem.1890.

[8] O. Welz, J. D. Savee, D. L. Osborn, S. S. Vasu, C. J. Percival, D. E. Shallcross, and C. A. Taatjes. “Direct Kinetic Measurements of Criegee Intermediate (CH_2OO) Formed by Reaction of CH_2I with O_2”. In: *Science* 335.6065 (2012), pp. 204–207. DOI: 10.1126/science.1213229.

[9] H. G. Kjœrgaard, T. Kurtén, L. B. Nielsen, S. Jørgensen, and P. O. Wennberg. “Criegee Intermediates React with Ozone”. In: *The Journal of Physical Chemistry Letters* 4.15 (2013), pp. 2525–2529. DOI: 10.1021/jz401205m.

[10] T. Berndt, T. Jokinen, M. Sipilä, R. L. M. III, H. Herrmann, F. Stratmann, H. Junninen, and M. Kulmala. “H_2SO_4 formation from the gas-phase reaction of stabilized Criegee Intermediates with SO_2: Influence of water vapour content and temperature”. In: *Atmospheric Environment* 89 (2014), pp. 603–612. ISSN: 1352-2310. DOI: 10.1016/j.atmosenv.2014.02.062.

[11] C. A. Taatjes, O. Welz, A. J. Eskola, J. D. Savee, A. M. Scheer, D. E. Shallcross, B. Rotavera, E. P. F. Lee, J. M. Dyke, et al. "Direct Measurements of Conformer-Dependent Reactivity of the Criegee Intermediate CH_3CHOO". In: *Science* 340.6129 (2013), pp. 177–180. DOI: 10.1126/science.1234689.

[12] C. A. Taatjes, G. Meloni, T. M. Selby, A. J. Trevitt, D. L. Osborn, C. J. Percival, and D. E. Shallcross. "Direct Observation of the Gas-Phase Criegee Intermediate (CH_2OO)". In: *Journal of the American Chemical Society* 130.36 (2008), pp. 11883–11885. DOI: 10.1021/ja804165q.

[13] J. M. Beames, F. Liu, L. Lu, and M. I. Lester. "Ultraviolet Spectrum and Photochemistry of the Simplest Criegee Intermediate CH2OO". In: *Journal of the American Chemical Society* 134.49 (2012), pp. 20045–20048. DOI: 10.1021/ja310603j.

[14] Y.-T. Su, Y.-H. Huang, H. A. Witek, and Y.-P. Lee. "Infrared Absorption Spectrum of the Simplest Criegee Intermediate CH2OO". In: *Science* 340.6129 (Apr. 2013), pp. 174–176. ISSN: 1095-9203. DOI: 10.1126/science.1234369.

[15] L. Vereecken and J. S. Francisco. "Theoretical studies of atmospheric reaction mechanisms in the troposphere". In: *Chemical Society Reviews* 41 (19 2012), pp. 6259–6293. DOI: 10.1039/C2CS35070J.

[16] D.-C. Fang and X.-Y. Fu. "CASSCF and CAS+1 + 2 Studies on the Potential Energy Surface and the Rate Constants for the Reactions between CH_2 and O_2". In: *The Journal of Physical Chemistry A* 106.12 (2002), pp. 2988–2993. DOI: 10.1021/jp014129m.

[17] M. T. Nguyen, T. L. Nguyen, V. T. Ngan, and H. M. T. Nguyen. "Heats of formation of the Criegee formaldehyde oxide and dioxirane". In: *Chemical Physics Letters* 448.4–6 (2007), pp. 183–188. ISSN: 0009-2614. DOI: 10.1016/j.cplett.2007.10.033.

[18] J. M. L. Martin and G. de Oliveira. "Towards standard methods for benchmark quality ab initio thermochemistry—W1 and W2 theory". In: *The Journal of Chemical Physics* 111.5 (1999), pp. 1843–1856. DOI: 10.1063/1.479454.

[19] A. Arneth, S. P. Harrison, S. Zaehle, K. Tsigaridis, S. Menon, P. J. Bartlein, J. Feichter, A. Korhola, M. Kulmala, et al. "Terrestrial biogeochemical feedbacks in the climate system". In: *Nature Geoscience* 3.8 (Aug. 2010), pp. 525–532. ISSN: 1752-0908. DOI: 10.1038/ngeo905.

[20] N. M. Donahue, G. T. Drozd, S. A. Epstein, A. A. Presto, and J. H. Kroll. "Adventures in Ozoneland: Down the Rabbit-hole". In: *Physical Chemistry Chemical Physics* 13 (23 2011), pp. 10848–10857. DOI: 10.1039/C0CP02564J.

[21] A. Karton, M. Kettner, and D. A. Wild. "Sneaking up on the Criegee intermediate from below: Predicted photoelectron spectrum of the CH_2OO^- anion and W3-F12 electron affinity of CH_2OO". In: *Chemical Physics Letters* 585 (Oct. 2013), pp. 15–20. ISSN: 0009-2614. DOI: 10.1016/j.cplett.2013.08.075.

[22] T. H. Dunning. "Gaussian basis sets for use in correlated molecular calculations. I. The atoms boron through neon and hydrogen". In: *The Journal of Chemical Physics* 90.2 (1989), pp. 1007–1023. DOI: 10.1063/1.456153.

[23] R. A. Kendall, T. H. Dunning, and R. J. Harrison. "Electron affinities of the first-row atoms revisited. Systematic basis sets and wave functions". In: *The Journal of Chemical Physics* 96.9 (1992), pp. 6796–6806. DOI: 10.1063/1.462569.

[24] CFOUR, a quantum chemical program package written by J.F. Stanton, J. Gauss, M.E. Harding, P.G. Szalay with contributions from A.A. Auer, R.J. Bartlett, U. Benedikt, C. Berger, D.E. Bernholdt, Y.J. Bomble, O. Christiansen, M. Heckert, O. Heun, C. Huber, T.-C. Jagau, D. Jonsson, J. Jusélius, K. Klein, W.J. Lauderdale, D.A. Matthews, T. Metzroth, D.P. O'Neill, D.R. Price, E. Prochnow, K. Ruud, F. Schiffmann, S. Stopkowicz, A. Tajti, J. Vázquez, F. Wang, J.D. Watts and the integral packages MOLECULE (J. Almlöf and P.R. Taylor), PROPS (P.R. Taylor), ABACUS (T. Helgaker, H.J. Aa. Jensen, P. Jørgensen, and J. Olsen), and ECP routines by A. V. Mitin and C. van Wüllen. For the current version, see http://www.cfour.de.

[25] H.-J. Werner, P. J. Knowles, G. Knizia, F. R. Manby, M. Schütz, et al. MOLPRO, *version 2012.1, a package of ab initio programs*. Cardiff, UK, 2012.

[26] A. Karton and J. M. L. Martin. "Explicitly correlated Wn theory: W1-F12 and W2-F12". In: *The Journal of Chemical Physics* 136.12, 124114 (2012), p. 124114. DOI: 10.1063/1.3697678.

[27] K. A. Peterson, D. Feller, and D. A. Dixon. "Chemical accuracy in ab initio thermochemistry and spectroscopy: current strategies and future challenges". In: *Theoretical Chemistry Accounts* 131.1 (2012), pp. 1–20. ISSN: 1432-881X. DOI: 10.1007/s00214-011-1079-5.

[28] S. Ten-no and J. Noga. "Explicitly correlated electronic structure theory from R12/F12 ansätze". In: *Wiley Interdisciplinary Reviews: Computational Molecular Science* 2.1 (2011), pp. 114–125. ISSN: 1759-0884. DOI: 10.1002/wcms.68.

[29] A. Karton, E. Rabinovich, J. M. L. Martin, and B. Ruscic. "W4 theory for computational thermochemistry: In pursuit of confident sub-kJ/mol predictions". In: *The Journal of Chemical Physics* 125.14, 144108 (2006), p. 144108. DOI: 10.1063/1.2348881.

[30] K. A. Peterson, T. B. Adler, and H.-J. Werner. "Systematically convergent basis sets for explicitly correlated wavefunctions: The atoms H, He, B–Ne, and Al–Ar". In: *The Journal of Chemical Physics* 128.8, 084102 (2008), p. 084102. DOI: 10.1063/1.2831537.

[31] G. Knizia and H.-J. Werner. "Explicitly correlated RMP2 for high-spin open-shell reference states". In: *The Journal of Chemical Physics* 128.15, 154103 (2008), p. 154103. DOI: 10.1063/1.2889388.

[32] T. B. Adler, G. Knizia, and H.-J. Werner. "A simple and efficient CCSD(T)-F12 approximation". In: *The Journal of Chemical Physics* 127.22, 221106 (2007), p. 221106. DOI: 10.1063/1.2817618.

[33] J. Noga, S. Kedžuch, and J. Šimunek. "Second order explicitly correlated R12 theory revisited: A second quantization framework for treatment of the operators' partitionings". In: *The Journal of Chemical Physics* 127.3, 034106 (2007), p. 034106. DOI: 10.1063/1.2751163.

[34] S. Ten-no. "Initiation of explicitly correlated Slater-type geminal theory". In: *Chemical Physics Letters* 398.1–3 (2004), pp. 56–61. ISSN: 0009-2614. DOI: 10.1016/j.cplett.2004.09.041.

[35] H.-J. Werner, G. Knizia, and F. R. Manby. "Explicitly correlated coupled cluster methods with pair-specific geminals". In: *Molecular Physics* 109.3 (2011), pp. 407–417. DOI: 10.1080/00268976.2010.526641.

[36] G. Knizia, T. B. Adler, and H.-J. Werner. "Simplified CCSD(T)-F12 methods: Theory and benchmarks". In: *The Journal of Chemical Physics* 130.5, 054104 (2009), p. 054104. DOI: 10.1063/1.3054300.

[37] K. A. Peterson and T. H. Dunning. "Accurate correlation consistent basis sets for molecular core–valence correlation effects: The second row atoms Al–Ar, and the first row atoms B–Ne revisited". In: *The Journal of Chemical Physics* 117.23 (2002), pp. 10548–10560. DOI: 10.1063/1.1520138.

[38] M. Douglas and N. M. Kroll. "Quantum electrodynamical corrections to the fine structure of helium". In: *Annals of Physics* 82.1 (1974), pp. 89–155. ISSN: 0003-4916. DOI: 10.1016/0003-4916(74)90333-9.

[39] B. A. Hess. "Relativistic electronic-structure calculations employing a two-component no-pair formalism with external-field projection operators". In: *Phys. Rev. A* 33 (6 June 1986), pp. 3742–3748. DOI: 10.1103/PhysRevA.33.3742.

[40] W. A. de Jong, R. J. Harrison, and D. A. Dixon. "Parallel Douglas–Kroll energy and gradients in NWChem: Estimating scalar relativistic effects using Douglas–Kroll contracted basis sets". In: *The Journal of Chemical Physics* 114.1 (2001), pp. 48–53. DOI: 10.1063/1.1329891.

[41] B. Ruscic, R. E. Pinzon, M. L. Morton, G. von Laszevski, S. J. Bittner, S. G. Nijsure, K. A. Amin, M. Minkoff, and A. F. Wagner. "Introduction to Active Thermochemical Tables: Several "Key" Enthalpies of Formation Revisited". In: *The Journal of Physical Chemistry A* 108.45 (2004), pp. 9979–9997. DOI: 10.1021/jp047912y.

[42] W. R. Stevens, B. Ruscic, and T. Baer. "Heats of Formation of $C_6H_5\cdot$, C_6H_5+, and C_6H_5NO by Threshold Photoelectron Photoion Coincidence and Active Thermochemical Tables Analysis". In: *The Journal of Physical Chemistry A* 114.50 (2010), pp. 13134–13145. DOI: 10.1021/jp107561s.

[43] B. Ruscic, R. E. Pinzon, M. L. Morton, N. K. Srinivasan, M.-C. Su, J. W. Sutherland, and J. V. Michael. "Active Thermochemical Tables: Accurate Enthalpy of Formation of Hydroperoxyl Radical, HO_2". In: *The Journal of Physical Chemistry A* 110.21 (2006), pp. 6592–6601. DOI: 10.1021/jp056311j.

[44] J. D. Cox, D. D. Wagman, and V. A. Medvedev. *CODATA Key Values for Thermodynamics*. see http://www.codata.org. New York, 1989.

[45] A. D. Becke. "Density-functional thermochemistry. III. The role of exact exchange". In: *The Journal of Chemical Physics* 98.7 (1993), pp. 5648–5652. DOI: 10.1063/1.464913.

[46] P. J. Stephens, F. J. Devlin, C. F. Chabalowski, and M. J. Frisch. "Ab Initio Calculation of Vibrational Absorption and Circular Dichroism Spectra Using Density Functional Force Fields". In: *The Journal of Physical Chemistry* 98.45 (1994), pp. 11623–11627. DOI: 10.1021/j100096a001.

[47] C. Lee, W. Yang, and R. G. Parr. "Development of the Colle-Salvetti correlation-energy formula into a functional of the electron density". In: *Physical Review B* 37 (2 Jan. 1988), pp. 785–789. DOI: 10.1103/PhysRevB.37.785.

[48] V. Mozhayskiy and A. Krylov. *ezSpectrum*.

[49] A. Karton, S. Daon, and J. M. Martin. "W4-11: A high-confidence benchmark dataset for computational thermochemistry derived from first-principles W4 data". In: *Chemical Physics Letters* 510.4–6 (2011), pp. 165–178. ISSN: 0009-2614. DOI: 10.1016/j.cplett.2011.05.007.

Supporting Information

Table S1 | CCSD(T) Optimised Geometries at from CCSD(T)/A'VTZ calculation.

	EO1: neutral *cis*-ethanal-oxide		
	x	*y*	*z*
C	−0.597 673	−0.679 246	0.000 000
H	−0.958 486	−1.701 138	0.000 000
O	0.676 240	−0.604 866	0.000 000
O	1.207 071	0.655 454	0.000 000
C	−1.427 923	0.537 996	0.000 000
H	−2.486 964	0.288 480	0.000 000
H	−1.162 820	1.145 816	0.871 687
H	−1.162 820	1.145 816	−0.871 687
	EO2: neutral *trans*-ethanal-oxide		
	x	*y*	*z*
C	−0.489 485	−0.428 951	0.000 000
H	−0.216 911	−1.481 387	0.000 000
O	0.469 175	0.402 657	0.000 000
O	1.744 408	−0.099 797	0.000 000
C	−1.879 766	0.095 051	0.000 000
H	−1.873 391	1.184 336	0.000 000
H	−2.415 299	−0.266 933	0.881 923
H	−2.415 299	−0.266 933	−0.881 923
	AEO1: anionic *cis*-ethanal-oxide		
	x	*y*	*z*
C	−0.634 608	0.682 744	−0.158 401
H	−1.056 198	1.638 224	0.165 511
O	0.689 823	0.656 521	0.095 975
O	1.253 705	−0.684 530	−0.042 937
C	−1.449 240	−0.560 551	0.047 675
H	−2.511 168	−0.320 638	−0.089 150
H	−1.159 227	−1.342 463	−0.656 091
H	−1.306 578	−0.985 528	1.056 384
	AEO2: anionic *trans*-ethanal-oxide		
	x	*y*	*z*
C	−0.504 603	0.462 235	−0.166 988
H	−0.220 527	1.444 238	0.209 318
O	0.452 856	−0.471 095	−0.073 743
O	1.780 206	0.133 052	0.087 515
C	−1.885 458	−0.077 265	0.091 903
H	−2.636 575	0.695 245	−0.103 910
H	−2.101 140	−0.929 797	−0.561 805
H	−2.024 023	−0.428 465	1.131 854

Cartesian Coordinates in Å

Figure S1 | Partial charges sourced from a natural population analysis calculation and projected onto the four ethanal-oxide oxide structures.

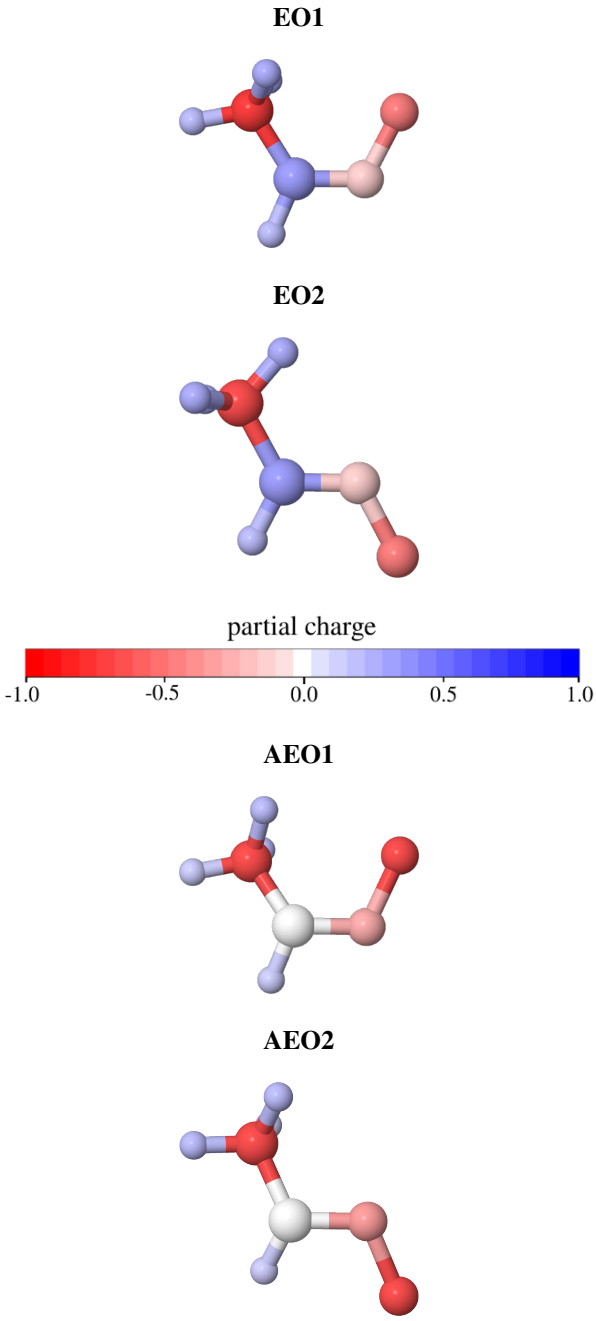

Table S2 | Orbital occupancies from NBO 6.0 calculations for the carbonyle oxide structures.

Molecule	**EO1**	**EO2**	**MO***	**AEO1**	**AEO2**	**AMO***
O_a lone pair	1.9718	1.9728	1.9780	2.9504	2.9474	2.9706
O_b lone pair	5.6964	5.7164	5.8510	5.8739	5.8978	5.9699
C_a lone pair	0.0000	0.0000	0.0000	0.9277	0.9149	0.9933
C_a–O_a bonding	3.9871	3.9848	3.9959	2.9866	2.9868	2.9960
C_a–C_b bonding	1.9953	1.9855	–	1.9947	1.9860	–
O_a–O_b bonding	1.9884	1.9852	1.9913	1.9872	1.9822	1.9873
C_a–O_b anti-bonding	0.3453	0.3158	0.1316	0.1214	0.0972	0.0180
C_a–C_b anti-bonding	0.0190	0.0126	–	0.0211	0.0148	–
O_a–O_b anti-bonding	0.0188	0.0159	0.0085	0.0183	0.0152	0.0088

* from Ref. [21]

Table S3 | Component breakdown of the W3-F12 total atomisation energies and heats of formation of the CH_3CHOO neutral and anion species (in kJ/mol) as well as the percentaged (T) contribution as an indicator for non-dynamic correlation.

Molecule	**AEO1**	**EO1**	**AEO2**	**EO2**
SCF	1860.0	1877.3	1866.8	1874.8
CCSD	949.6	907.9	944.1	897.2
(T)	79.8	88.3	78.8	85.9
T_3 − (T)	−3.6	−4.6	−3.6	−4.2
(Q)	5.5	9.9	5.2	9.9
Inner-Shell	10.0	10.6	10.1	10.6
Scalar Relativistic	−3.0	−2.6	−3.0	−2.7
Spin-Orbit	−2.6	−2.6	−2.6	−2.6
DBOC	0.4	0.6	0.4	0.6
TAE_e	2896.2	2884.7	2896.2	2869.6
ZPVE	147.8	155.4	147.3	154.4
TAE_0	2748.4	2729.3	2748.8	2715.2
$\Delta H_{f,0}$	32.2	51.3	31.7	65.4
$\Delta H_{f,298}$	20.1	37.8	20.0	52.6
%TAE[(T)]	2.8	3.1	2.7	3.0

Figure S2 | Predicted Gaussian convoluted anion photoelectron spectra for both transitions (full width at half maximum is 0.002 eV).

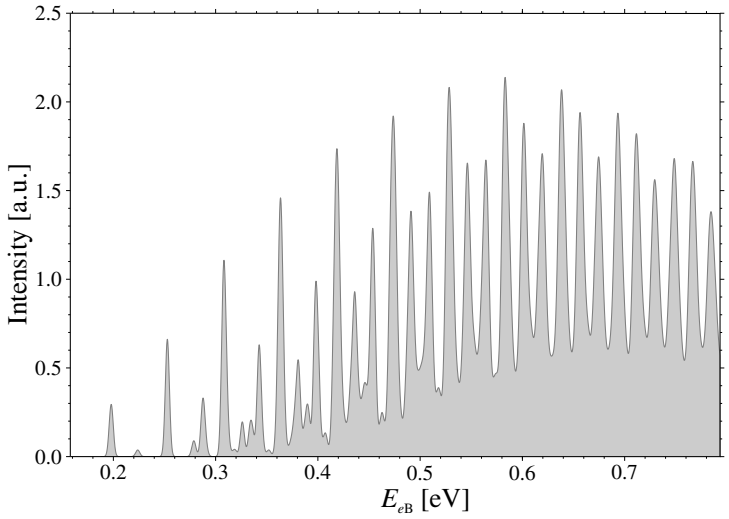

T1: EO1 ← AEO1

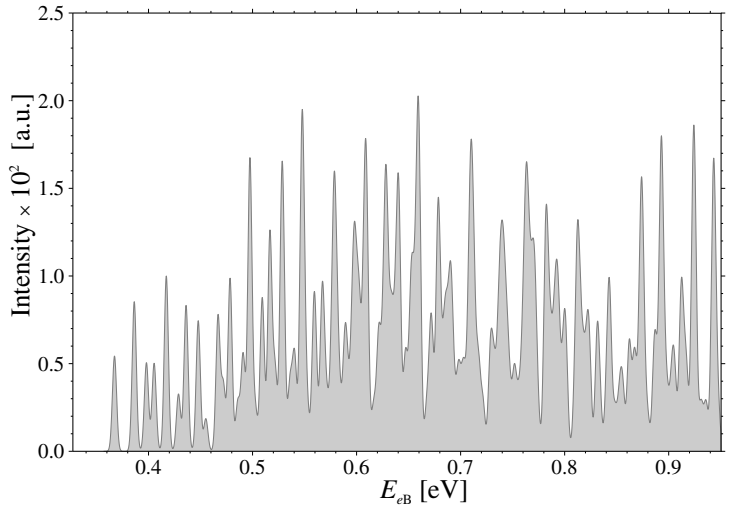

T2: EO2 ← AEO2